

Platinum fluorides beyond PtF₆?

Sebastian Riedel

Department of Chemistry, University of Helsinki, A.I. Virtasen aukio 1, FIN-00014 Helsinki, Finland

Received 26 February 2007; received in revised form 28 March 2007; accepted 2 April 2007

Available online 6 April 2007

Abstract

Quantum-chemical calculations at DFT B3LYP and ab initio MP2, CCSD, and CCSD(T) levels have been performed on various binary fluorides of platinum up to formal oxidation state +VIII, to evaluate the stability of these species. The calculations indicate clearly that elimination of F₂ from PtF₈ is a strongly exothermic reaction, with a moderate activation barrier. An exothermic decay is also observed for the homolytic bond breaking. Furthermore, our investigations suggest that both decomposition channels of PtF₇ are exothermic. The existence of platinum fluorides higher than PtF₆ is therefore highly unlikely.

© 2007 Elsevier B.V. All rights reserved.

Keywords: Platinum fluorides; High oxidation states; Transition states; Thermochemistry; Electron affinity; Coupled-cluster calculations; Density functional theory

1. Introduction

Transition metals in high oxidation states are still of interest, not least because these species can be used as powerful oxidisers or fluorination agents in all areas of chemistry [1,2]. As we have recently shown for the 5d transition metals, the highest attainable formal oxidation state increase with the group number up to group 8 (osmium) thereafter we observe a linear descent through group 12 (mercury), see Fig. 1 [3]. This linear trend can also be observed by taking only transition metal fluorides into account [4]. To prove this prediction of a linear behavior for the 5d transition metal fluorides we study the stabilities of higher binary platinum fluorides up to PtF₈.

The highest experimentally known oxidation state of platinum that is characterised beyond doubt is +VI, for example in PtF₆ [5,6]. Even in a matrix-isolation experiment, using oxygen as a ligand, no higher oxidation state than +VI (Pt(OO)O₂ or PtO₃) could be observed [7]. Platinum fluorides up to formal oxidation state +VIII have already been reported by Schwerdtfeger and co-worker using high-level quantum-chemical calculations [8,9]. In this study only even numbers of platinum fluorides were investigated PtF_{*n*} (*n* = 2, 4, 6, 8). However, for a complete review of the highest possible

platinum oxidation states we also have to consider platinum heptafluoride.

In the present study we investigate higher binary platinum fluorides up to formal oxidation state +VIII by high-level quantum-chemical calculations up to and including CCSD(T) level. We report molecular structures, gas-phase elimination reactions, transition states and electron affinities to investigate the stabilities of these species.

2. Results and discussion

2.1. PtF₈

Fig. 2 shows the optimised molecular structures of the platinum octafluoride, PtF₈. We found two minima for the singlet PtF₈ species. One minimum is a square antiprism with *D*_{4d} symmetry, this is in agreement with previous results of Schwerdtfeger and co-worker [8]. The corresponding triplet spin state lies 109.9 kJ mol⁻¹ (B3LYP) above the *D*_{4d} singlet minimum. The calculated Pt–F bond distance of 192.2 pm is slightly shorter than the previous value of 193.7 pm [8], see Table 1. The other optimised minimum is a square prism showing *D*_{4h} symmetry, see Fig. 2. The Pt–F bond distance (195.4 pm) is only 3.2 pm longer than the bond distance of the square antiprism. The energies of these two minima differ by 151.5 kJ mol⁻¹ preferring the square antiprism. This result is in

E-mail address: sebastian.riedel@psichem.de.

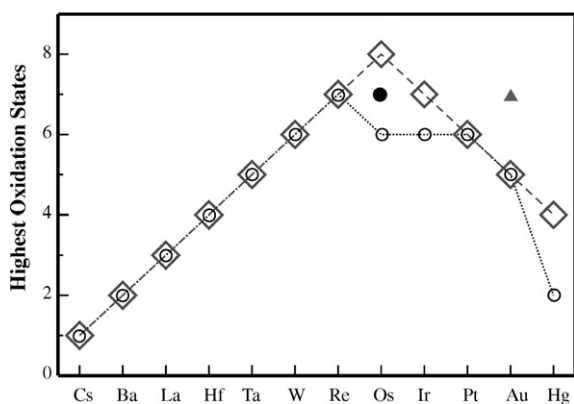


Fig. 1. The maximum formal oxidation states of binary 5d transition metal fluorides: (○) highest experimentally known MF_n species, (▲) incorrect experimental assignment, (●) controversial experimental assignment but quantum-chemically predicted and (◇) suggested maximum achievable oxidation states.

agreement with a previous study of octafluorides by Seppelt and co-worker [10,11]. The square antiprism can be called ideal when the α -angle ($\text{F-M-z}_{\text{axis}}$) is measured to be 57.1° , as it is defined in Refs. [10,11]. For the PtF_8 species we observe an α -angle of 57.7° slightly larger than the ideal one. For comparison, the cubic PtF_8 structure shows an α -angle of 56.1° .

The other common structure for coordination number eight is a triangular dodecahedron, of symmetry D_{2d} [11]. This structure is found to be a transition state and lies 18.1 kJ mol^{-1} above the square antiprism (imaginary frequency of $i125.5 \text{ cm}^{-1}$).

Unimolecular gas-phase F_2 -elimination from PtF_8 to give PtF_6 is found to be exothermic at all quantum-chemical levels used, see Table 2. This is again in good agreement with previous results from Schwerdtfeger and Wesendrup [8]. The corresponding barrier for a concerted F_2 -elimination at B3LYP level is calculated to be 86.0 kJ mol^{-1} . The optimised transition state has C_2 symmetry. Another potential channel for decomposition of PtF_8 involves the homolytic dissociation $\text{PtF}_8 \rightarrow \text{PtF}_7 + \text{F}$. This reaction is also computed to be exothermic by $-73.4 \text{ kJ mol}^{-1}$ at B3LYP level, Table 2. Due to substantial nuclear reorganisations the homolytic bond breaking of higher coordinated metal fluorides can show appreciable barriers [3,12]. The transition state for the homolytic bond breaking of the PtF_8 species could unfortunately not be located. We were

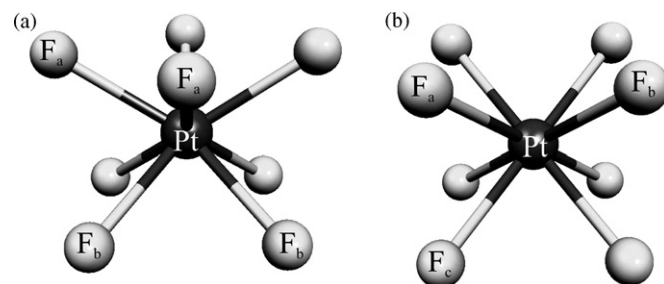


Fig. 2. B3LYP-optimised minimum structures of PtF_8 . (a) Square antiprism (D_{4d}) and (b) prism (D_{4h}).

Table 2
Computed reaction energies (in kJ mol^{-1})^a

Reaction	B3LYP ^b	ZPE ^c	MP2	CCSD	CCSD(T) ^d
$\text{PtF}_8 \rightarrow \text{PtF}_6 + \text{F}_2$ ^e	-306.4		-90.2	-304.4	-229.7
$\text{PtF}_8 \rightarrow \text{PtF}_6 + \text{F}_2$	-306.0 (86.0)	-313.3	-130.3	-310.7	-248.3
$\text{PtF}_8 \rightarrow \text{PtF}_7 + \text{F}$	-73.4	-83.7	-43.5	-120.5	-154.1
$2\text{PtF}_8 \rightarrow 2\text{PtF}_7 + \text{F}_2$	-302.1 (52.9)	-316.5	-409.6	-688.0	-908.0
$\text{PtF}_7 \rightarrow \text{PtF}_5 + \text{F}_2$	-26.7 (77.2)	-32.3	38.4	-74.6	-116.1
$\text{PtF}_7 \rightarrow \text{PtF}_6 + \text{F}$	-77.3 (4.6)	-80.5	-77.5	-186.8	-248.7
$2\text{PtF}_7 \rightarrow 2\text{PtF}_6 + \text{F}_2$	-309.9	-310.1	-477.6	-820.6	-1097.2

^a Reaction energies for singlet PtF_8 , doublet PtF_7 , triplet PtF_6 and doublet PtF_5 .

^b Values in parentheses are barriers for the corresponding reaction.

^c Zero-point vibration corrected energies (B3LYP level) using the DZ + P basis set for fluorine.

^d T_1 -diagnostics: PtF_8 (0.020), PtF_7 (0.029), PtF_6 (0.034), PtF_5 (0.029).

^e Values are thermochemical data of Ref. [8].

however able to find the imaginary frequency which matches the homolytic bond breaking by scanning the potential energy surface. This point lies 110 kJ mol^{-1} above the PtF_8 minimum structure. Note that, this point is not corresponding to a real transition state and optimisations of this structure always lead to some other stationary point with several imaginary frequencies. However, it allows us to estimate, that there exists a barrier for the homolytic bond breaking. Furthermore, our attempts to calculate the transition state of the bimolecular reaction $2\text{PtF}_8 \rightarrow 2\text{PtF}_7 + \text{F}_2$ were successful. The transition state shows C_{2v} symmetry and the related imaginary frequency is computed to be $i435.3 \text{ cm}^{-1}$. This transition state corresponds to two-homolytic bond breakings forming a new F–F

Table 1
Molecular structures (minima) of platinum fluorides optimised at B3LYP level

PtF_8 , D_{4d}	B3LYP	PtF_8 , D_{4h}	B3LYP	PtF_7^a , C_{2v}	B3LYP	PtF_7^b , C_{2v}	B3LYP	PtF_6 , D_{4h}	B3LYP	PtF_5 , C_{4v}	B3LYP
Pt–F	192.2	Pt–F	195.4	$\text{F}_{\text{ax}}\text{–Pt}$	187.9	$\text{F}_{\text{ax}1}\text{–Pt}$	187.5	$\text{F}_{\text{ax}}\text{–Pt}$	185.2	$\text{F}_{\text{ax}}\text{–Pt}$	199.0
$\text{F}_a\text{–Pt–F}_a$	73.4	$\text{F}_a\text{–Pt–F}_b$	71.9	$\text{F}_{\text{eq}1}\text{–Pt}$	189.5	$\text{F}_{\text{ax}2}\text{–Pt}$	193.5	$\text{F}_{\text{eq}}\text{–Pt}$	187.7	$\text{F}_{\text{eq}}\text{–Pt}$	187.9
$\text{F}_b\text{–Pt–F}_b$	73.4	$\text{F}_a\text{–Pt–F}_c$	67.8	$\text{F}_{\text{eq}2}\text{–Pt}$	191.7	$\text{F}_{\text{eq}}\text{–Pt}$	188.8			$\text{F}_{\text{ax}}\text{–Pt–F}_{\text{eq}}$	98.1
$\text{F}_a\text{–Pt–F}_b$	77.3	$\text{F}_b\text{–Pt–F}_c$	108.1	$\text{F}_{\text{eq}3}\text{–Pt}$	190.3	$\text{F}_{\text{eq}}\text{–Pt–F}_{\text{ax}1}$	81.8			$\text{F}_{\text{eq}}\text{–Pt–F}_{\text{eq}}$	88.9
				$\text{F}_{\text{ax}}\text{–Pt–F}_{\text{ax}}$	180.0	$\text{F}_{\text{ax}1}\text{–Pt–F}_{\text{ax}2}$	144.6				
				$\text{F}_{\text{eq}1}\text{–Pt–F}_{\text{eq}2}$	72.0						
				$\text{F}_{\text{eq}2}\text{–Pt–F}_{\text{eq}3}$	72.0						

Bond distances in pm and angles in degrees.

^a Molecular structure of the distort pentagonal bipyramid.

^b Transition state of the monocapped trigonal prism.

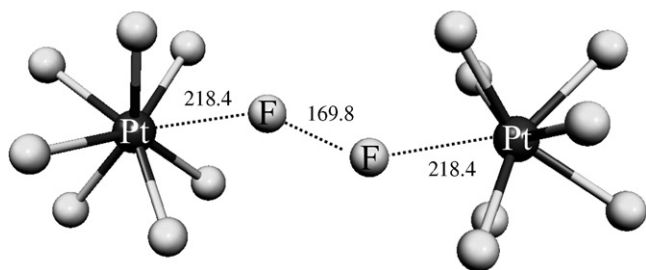


Fig. 3. B3LYP-optimised transition state (C_{2v} symmetry) of the bimolecular elimination reaction $2\text{PtF}_8 \rightarrow 2\text{PtF}_7 + \text{F}_2$. Bond distances in pm.

bond, see Fig. 3. The barrier for this elimination is calculated to be 52.9 kJ mol^{-1} at B3LYP level. The bimolecular F_2 -elimination energy is computed to be strongly exothermic by $-302.1 \text{ kJ mol}^{-1}$ at B3LYP level, see Table 2.

2.2. PtF_7

If one fluorine is omitted the next structure would be the homoleptic platinum fluoride PtF_7 , shown in Fig. 4. The PtF_7 (doublet ground state) exhibits a distorted pentagonal bipyramidal minimum structure with C_{2v} symmetry. This structure is in line with several other experimental and calculated heptafluorinated transition metals, e.g., ReF_7 [13], OsF_7 [4], IrF_7 [3], AuF_7 [12]. The molecular structure shows a Jahn–Teller compression with a $\text{Pt}-\text{F}_{\text{ax}}$ bond distance of 187.9 pm at B3LYP level. Apart from the pentagonal bipyramid, two further VSEPR coordination polyhedra for hepta-coordinated neutral atom are known [14]. The monocapped trigonal prism (C_{2v}) is calculated to be a transition state (with an imaginary frequency of $i97.6 \text{ cm}^{-1}$) 22.2 kJ mol^{-1} above the distorted pentagonal bipyramidal structure. All attempts to locate the last missing VSEPR structure, the monocapped octahedron (C_{3v}), led back to the distorted pentagonal bipyramidal structure 4a.

The concerted gas-phase F_2 -elimination $\text{PtF}_7 \rightarrow \text{PtF}_5 + \text{F}_2$ shows an exothermic decomposition channel of $-26.7 \text{ kJ mol}^{-1}$, see Table 2. Attempts to calculate the transition state and the corresponding barrier for the concerted F_2 -elimination led to a C_{2v} transition state 77.2 kJ mol^{-1} above the PtF_7 minimum. Calculation of the homolytic $\text{Pt}-\text{F}$ bond splitting indicates an even more exothermic pathway than for the concerted F_2 -elimination. The F -elimination is computed to be

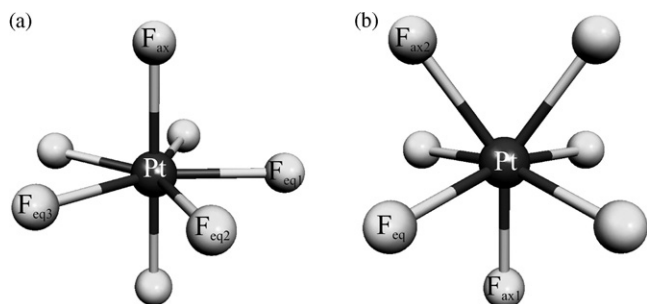


Fig. 4. B3LYP-optimised structures of PtF_7 . (a) Minimum distorted pentagonal bipyramidal (C_{2v}) and (b) transition state monocapped trigonal prism (C_{2v}).

exothermic by $-77.3 \text{ kJ mol}^{-1}$ at B3LYP level. The barrier for the homolytic bond breaking is only 4.6 kJ mol^{-1} . Such a very low barrier, together with the exothermic decomposition channel of the homolytic bond breaking indicates that the elimination reaction is the preferred decomposition channel of the PtF_7 species.

Our calculations of the bimolecular F_2 -elimination $2\text{PtF}_7 \rightarrow 2\text{PtF}_6 + \text{F}_2$ show a strongly exothermic reaction channel of $-309.9 \text{ kJ mol}^{-1}$ at B3LYP level, see Table 2.

2.3. PtF_6 and PtF_5

In agreement with the previous theoretical study [8] of platinum fluoride species, we found the triplet ground state configuration of the PtF_6 minimum to be a distorted octahedron (without considering spin-orbit coupling). This is due to a Jahn–Teller effect which will shorten the F_{ax} bond distance by 2.5 pm leading to a D_{4h} structure. The singlet lies 72.6 kJ mol^{-1} higher in energy than the triplet ground state. Note that, PtF_6 is experimentally characterised to be regular octahedral (O_h symmetry) in the gas-phase [15–17] and in the solid state [18]. This small discrepancy between our calculations and the experimental results might be due to a spin-orbit effect (SO) which generates a $t_{3/2}^4$ singlet ground-state [18]. However, a more stabilised PtF_6 species would lead to more exothermic decomposition channels and therefore destabilises higher platinum fluorides. This SO effect of PtF_6 is still under study and will be reported elsewhere. For more detailed discussion of platinum hexafluorides see Refs. [8,18].

Monomeric PtF_5 is calculated to show a C_{4v} symmetrical doublet minimum, see Fig. 5. The quartet-doublet gap amounts to 59.9 kJ mol^{-1} . The structural unit of platinum metal pentafluorides is a tetramer with bridging fluorine atoms in *cis* position [19–21]. This oligomerisation of PtF_5 monomers will favour the F_2 -elimination of PtF_7 due to the larger stability of the tetramers as compared to the monomers. The evaluation of this effect is outside the scope of the present work.

2.4. Electron affinities

The electron affinity can be used as an indicator of the stability of species with metals in higher oxidation states. Therefore, we have computed vertical (VEA) and adiabatic electron affinities (AEA) of binary platinum fluorides. They are

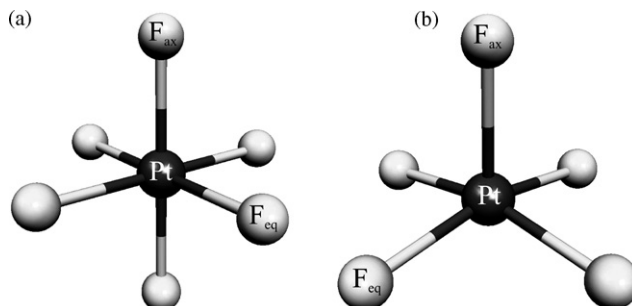


Fig. 5. B3LYP-optimised minimum structures of PtF_6 and PtF_5 . (a) Octahedral PtF_6 structure (D_{4h}) and (b) square pyramidal PtF_5 structure (C_{4v}).

Table 3
Computed adiabatic electron affinities (AEA) in eV

EA	B3LYP	MP2	CCSD	CCSD(T)	T ₁ -diagnostic ^a	Experimental
PtF ₆ ^b (VEA) ^c	8.66	7.57	7.01	6.68		
PtF ₆ ^b	6.78	6.43	7.43	6.95		7.00 ± 0.35 ^d
PtF ₆ ^c	6.80	6.50	7.48	6.99	0.030 (0.025)	
PtF ₇ (VEA) ^c	7.27	7.30	8.25	7.68	0.029 (0.020)	
PtF ₇	7.37	7.34 ^f	8.17 ^f	7.68 ^f	0.029 (0.020)	
PtF ₈ (VEA) ^c	6.47	5.90	6.57	6.16	0.020 (0.020)	
AuF ₆ ^c	8.13	8.38	9.01	8.52	0.020 (0.034)	
AuF ₆ ^c	8.06	8.33	8.96	8.47	0.021 (0.034)	

^a T₁-diagnostics (in parentheses for the anionic species).

^b Ref. [8].

^c Vertical electron affinities.

^d Ref. [34].

^e Ref. [12].

^f Single-point calculations at B3LYP optimised structures.

shown in Table 3. It is clearly seen that our calculated EA of the PtF₆ species are in excellent agreement with the previous calculated and experimentally measured electron affinities. We believe that our computed electron affinities for the higher platinum fluorides are of the same order of accuracy.

It is interesting to note that the EA for the PtF₇ is the highest calculated EA of all platinum fluorides. Such extraordinary EA of 7.68 eV at CCSD(T) level would characterise the hypothetical PtF₇ species as one of the strongest oxidisers known. Until now, only the hypothetical AuF₆ species has shown an even higher EA of 8.5 eV [12]. As reported before, the electron affinity of the PtF₈ species is calculated to be 6.16 eV at CCSD(T) level and is therefore below the EA of the PtF₆ species. It seems that the F₂-elimination of the anionic [PtF₈]⁻ species is even more exothermic than the elimination of the PtF₈.

3. Computational methods

Molecular structures were optimised using density-functional theory (hybrid B3LYP functional) [22–25] with the Gaussian03 [22] program. Transition-state optimisations were done using synchronous transit-guided quasi-Newton (STQN) methods using the QST2 and QST3 keywords in Gaussian03 [26,27]. Optimisations were followed by single-point energy calculations at the DFT, MP2, and high-level coupled-cluster (CCSD and CCSD(T)) levels. Quasirelativistic, energy-adjusted, small-core “Stuttgart-type” pseudo-potentials (effective-core potentials, ECPs) were used for the platinum metal [28]. The corresponding (8s7p6d)[6s5p3d] valence basis set for Pt was augmented by one f-type polarisation function [29] (α_f : Pt 0.993). In the B3LYP-optimisations, a fluorine DZ + P all-electron basis set by Dunning was used [30].

Stationary points on the potential energy surface were characterised by harmonic vibrational frequency analyses at the B3LYP level (providing also zero-point energy corrections to the thermochemistry). Subsequent single-point energy calculations had the fluorine basis replaced by a larger aug-cc-pVTZ basis set [31]. The post-HF calculations were carried out with the MOLPRO 2006.1 program package [32]. Basis-set super-

position errors (BSSE) were not estimated, as they were found to be small (5–10 kJ mol⁻¹) in previous studies [3,4,12,33].

We have computed vertical (VEA) and adiabatic electron affinities (AEA). The VEA correspond to a single-point calculation of the anionic species using the geometry of the neutral one. For AEA we have also optimised the anionic structure at the B3LYP level.

Note, that the methodology used here, in particular B3LYP optimisations followed by B3LYP or CCSD(T) single-point energy calculations with larger basis sets, are well established as a reliable tool for redox thermochemistry in the 5d transition metal series, e.g. in previous studies on Hg [33], Au [12], Pt [8], and Ir [3] systems. Furthermore, we found excellent agreement between theory and experiment for structures and relevant thermochemical data in test calculations of ReF₇. The results will be reported elsewhere as part of a wider computational study. Spin-orbit corrections are not considered in this work.

4. Conclusions

The evaluation of molecular structures and gas-phase stabilities of higher binary platinum fluorides up to formal oxidation state + VIII indicates that no higher fluorides like PtF₇ or PtF₈ should exist. We have shown that all possible decomposition channels of the PtF₈ species are exothermic. Even though there is a moderate barrier calculated for the concerted F₂-elimination, the barrier for the bimolecular homolytic bond breaking (2PtF₈ → 2PtF₇ + F₂) is rather low (52.9 kJ mol⁻¹). Furthermore, our high level quantum-chemical calculations up to CCSD(T) level indicated that the platinum heptafluoride is a very unstable species. Both elimination reactions, the concerted and the homolytic bond breaking, are exothermic. The barrier of the last mentioned reaction is vanishingly small and PtF₇ thus easily eliminates a fluorine atom. To conclude: due to exothermic reaction channels with small elimination barriers it is therefore most unlikely that higher platinum fluorides will ever be experimentally observed. Our previous prediction of a linear trend for the 5d transition metal fluorides has been verified [3,4].

Acknowledgments

The author is grateful to P. Pyykkö, M. Kaupp, D. Sundholm, M. Straka and M. Patzschke for stimulating discussions and for provided computational resources. This work was supported by the Alexander von Humboldt Foundation (Feodor Lynen Research Fellowship). This project belongs to the Finnish CoE in Computational Molecular Science.

References

- [1] N. Bartlett, *Angew. Chem. Int. Ed.* 7 (1968) 433–439.
- [2] K.O. Christe, W.W. Wilson, R.D. Wilson, *Inorg. Chem.* 23 (1984) 2058–2063.
- [3] S. Riedel, M. Kaupp, *Angew. Chem. Int. Ed.* 45 (2006) 3708–3711.
- [4] S. Riedel, M. Kaupp, *Inorg. Chem.* 45 (2006) 10497–10502.
- [5] B. Weinstock, H.H. Claassen, J.G. Malm, *J. Am. Chem. Soc.* 79 (1957) 5832.
- [6] N. Bartlett, D.H. Lohmann, *J. Chem. Soc.* (1964) 619–626.
- [7] W.D. Bare, A. Citra, G.V. Chertihin, L. Andrews, *J. Phys. Chem. A* 103 (1999) 5456–5462.
- [8] R. Wesendrup, P. Schwerdtfeger, *Inorg. Chem.* 40 (2001) 3351–3354.
- [9] The result of this study was recently incorrectly cited as it was claimed that PtF_8^- would be a stable species G. Aullon, S. Alvarez, *Inorg. Chem.* 46 (2007) 2700–2703.
- [10] I.C. Hwang, K. Seppelt, *J. Fluorine Chem.* 102 (2000) 69–72.
- [11] D.L. Kepert, *Stereochemistry, Inorganic Chemistry Concepts*, vol. 6, Springer, Berlin, 1982.
- [12] S. Riedel, M. Kaupp, *Inorg. Chem.* 45 (2006) 1228–1234.
- [13] T. Vogt, A.N. Fitch, J.K. Cockcroft, *Science* 263 (1994) 1265–1267.
- [14] R. Hoffmann, B.F. Beier, E.L. Muetterties, A.R. Rossi, *Inorg. Chem.* 16 (1977) 511–522.
- [15] S.V. Zemskov, S.P. Gabuda, *Zh. Strukt. Khim.* 17 (1976) 904–921.
- [16] B. Weinstock, *Physics and Chemistry of Solids* 18 (1961) 86–89.
- [17] R. Glauber, V. Schomaker, *Phys. Rev.* 89 (1953) 667–671.
- [18] T. Drews, J. Supel, A. Hagenbach, K. Seppelt, *Inorg. Chem.* 45 (2006) 3782–3788.
- [19] A.V. Dzhilavyan, E.G. Rakov, A.S. Dudin, *Usp. Khim.* 52 (1983) 1676–1697.
- [20] S. Cotton, *Chemistry of Precious Metals*, Chapman & Hall, Weinheim, 1997.
- [21] A.F. Holleman, E. Wiberg, 71–101th ed., *Lehrbuch der Anorganischen Chemie*, vol. 101, Walter de Gruyter, Berlin, 1995.
- [22] M.J. Frisch, G.W. Trucks, H.B. Schlegel, G.E. Scuseria, M.A. Robb, J.R. Cheeseman, J.A. Montgomery, J.T. Vreven, K.N. Kudin, J.C. Burant, J.M. Millam, S.S. Iyengar, J. Tomasi, V. Barone, B. Mennucci, M. Cossi, G. Scalmani, N. Rega, G.A. Petersson, H. Nakatsuji, M. Hada, M. Ehara, K. Toyota, R. Fukuda, J. Hasegawa, M. Ishida, T. Nakajima, Y. Honda, O. Kitao, H. Nakai, M. Klene, X. Li, J.E. Knox, H.P. Hratchian, J.B. Cross, C. Adamo, J. Jaramillo, R. Gomperts, R.E. Stratmann, O. Yazyev, A.J. Austin, R. Cammi, C. Pomelli, J.W. Ochterski, P.Y. Ayala, K. Morokuma, G.A. Voth, P. Salvador, J.J. Dannenberg, V.G. Zakrzewski, S. Dapprich, A.D. Daniels, M.C. Strain, O. Farkas, D.K. Malick, A.D. Rabuck, K. Raghavachari, J.B. Foresman, J.V. Ortiz, Q. Cui, A.G. Baboul, S. Clifford, J. Cioslowski, B.B. Stefanov, G. Liu, A. Liashenko, P. Piskorz, I. Komaromi, R.L. Martin, D.J. Fox, T. Keith, M.A. Al-Laham, C.Y. Peng, A. Nanayakkara, M. Challacombe, P.M.W. Gill, B. Johnson, W. Chen, M.W. Wong, C. Gonzalez, J.A. Pople, Revision B.04 ed., Pittsburgh, PA, 2003.
- [23] A.D. Becke, *J. Chem. Phys.* 98 (1993) 5648–5652.
- [24] C. Lee, W. Yang, R.G. Parr, *Phys. Rev. B* 37 (1988) 785–789.
- [25] B. Miehlich, A. Savin, H. Stoll, H. Preuss, *Chem. Phys. Lett.* 157 (1989) 200–206.
- [26] C. Peng, H.B. Schlegel, *Isr. J. Chem.* 33 (1994) 449–454.
- [27] C. Peng, P. Ayala, H.B. Schlegel, M.J. Frisch, *J. Comput. Chem.* 17 (1996) 49–56.
- [28] D. Andrae, U. Häussermann, M. Dolg, H. Stoll, H. Preuss, *Theor. Chim. Acta* 77 (1990) 123–141.
- [29] A.W. Ehlers, M. Bohme, S. Dapprich, A. Gobbi, A. Hollwarth, V. Jonas, K.F. Kohler, R. Stegmann, A. Veldkamp, G. Frenking, *Chem. Phys. Lett.* 208 (1993) 111–114.
- [30] T.H. Dunning Jr., *J. Chem. Phys.* 53 (1970) 2823–2833.
- [31] T.H. Dunning Jr., *J. Chem. Phys.* 90 (1989) 1007–1023.
- [32] H.-J. Werner, P.J. Knowles, R. Lindh, F.R. Manby, M. Schütz, P. Celani, T. Korona, G. Rauhut, R.D. Amos, A. Bernhardsson, A. Berning, D.L. Cooper, M.J.O. Deegan, A.J. Dobbyn, F. Eckert, C. Hampel, G. Hetzer, A.W. Lloyd, S.J. McNicholas, W. Meyer, M.E. Mura, A. Nicklaß, P. Palmieri, R. Pitzer, U. Schumann, H. Stoll, A.J. Stone, R. Tarroni, T. Thorsteinsson, *MOLPRO 2006.1 ed.*, Birmingham, UK, 2006.
- [33] S. Riedel, M. Straka, M. Kaupp, *Phys. Chem. Chem. Phys.* 6 (2004) 1122–1127.
- [34] M.V. Korobov, S.V. Kuznetsov, L.N. Sidorov, V.A. Shipachev, V.N. Mit'kin, *Int. J. Mass Spectrom. Ion Process.* 87 (1989) 13–27.